STM JOURNALS

Journal of
Polymer & Composites

ISSN: 2321-2810 (Online)
ISSN: 2321-8525 (Print)
Volume 14, Issue 3, 2026
DOI (Journal): 10.37591/JoPC

https://journals.stmjournals.com/jopc

Research JoPC

Interfacial Engineering of Carbon Fiber/Epoxy Laminates Using Functionalized Graphene Nanoplatelets: Experimental and Numerical Study

Sandip K. Kadu[1*], Palash Soni[2], Shripad R. Nimbalkar[3]

Abstract

Current research work studies the influence of amines(–NH_2) and carboxyl(–COOH) functionalized graphene nanoplatelets on the mechanical and thermomechanical behavior of unidirectional hybrid composite. Composites having different graphene concentration from 0 to 0.7 wt% were fabricated, characterized and analyzed for multiple testing - tensile testing, dynamic mechanical analysis (DMA) and Fourier transform infrared spectroscopy (FTIR). Tensile testing indicates better elastic modulus and tensile strength due to efficient load transfer between nanoparticles fiber and matrix with most improved properties at 0.5% graphene. Finite element analysis has been performed to simulate orthotropic laminate properties and maximum-stress first-ply failure theory generates the experimental stress–strain response and failure load, with deviations within 5%. DMA indicates increase in storage modulus and elevation in glass transition temperature(T_g), which improves interfacial bonding and better polymer chain mobility due to graphene reinforcement. Functionalization improves dispersion and interfacial bonding. Amine functionalized graphene nanoparticles (GNP) results in minor better modulus. The maximum flexural stress of the composite specimen was equal to the corresponding stress of the peak force before the failure of the specimen and flexural strength of hybrid layered composite evaluated for o.5% wt. fraction of GnP. In totality, the combined experimentation and FEA approach demonstrates that functionalized GNP improves mechanical and thermomechanical properties of carbon fiber reinforced polymer.

Keywords: Multi-phase composite, Mechanical characterisation, Functionalisation, GnP, Glass transition temperature, Loss modulus

INTRODUCTION

As industries like aerospace, defense, automotive, and high-performance electronics push for materials that are lighter, stronger, and more heat-resistant, advanced polymer composites have gained a lot of attention. Among these, carbon fiber reinforced polymers (CFRP) continue to lead the way. They are widely used because they offer an excellent balance of strength and stiffness while remaining lightweight, along with good fatigue resistance and the flexibility to be tailored for different design needs. [1], [2]. In addition, even though conventional CFRP are widely used, their performance is often restricted by poor interfacial bonding. The inertness of carbon fiber makes it difficult during bonding it with epoxy matrix. This makes the ineffective transfer of load, stress, occurrence of damage, early cause of interfacial breakage and simultaneously drastic effect over

***Author for Correspondence**
Sandip K. Kadu

[1]Research Scholar, Department of Mechanical Engineering, Oriental University, Indore, Madhya Pradesh, India
[2]Assistant Professor, Department of Mechanical Engineering, Oriental University, Indore, Madhya Pradesh, India
[3]Assistant Professor, Mechanical engineering, Pravara Rural Engineering College, Loni, Maharashtra, India

Received Date: April 15, 2026
Accepted Date: April 22, 2026
Published Date: May 07, 2026

Citation:
Sandip K. Kadu, Palash Soni, Shripad R. Nimbalkar. Interfacial Engineering of Carbon Fiber/Epoxy Laminates Using Functionalized Graphene Nanoplatelets: Experimental and Numerical Study. Journal of Polymer & Composites. 2026; 14(3): 61–77p.

thermo-mechanical loading and performance [3], [4]. To avoid these difficulties the researchers were start working on nano reinforcements. These generally happens due to drastic difference between the elastic property of matrix and reinforcement, which is managed by addition of nanoscale reinforcements in matrix. Due to addition of nanofillers in two-phase composites, researchers showed that improvement occurs in properties, load and stress transfer capacity, and so thermomechanical loading behaviour [5], [6], [7]. The researchers were start working on various nanofillers and observe that graphene nanoplatelets (GnP) will give required outcomes, as it exhibit higher elastic modulus of 1Tpa and tensile strength of 130 GPa with good thermal conductivity of around 3000 $Wm^{-1}K^{-1}$[7], [8], [9].

. From a structural point of view, GNP are made up of a few layers of graphene arranged in a 2D form with a high aspect ratio. This geometry provides a much larger interfacial contact area, especially when compared to one-dimensional fillers like carbon nanotubes(CNT) [10], [11], [12]. Because of this unique geometry, GNP are especially effective in redistributing stress within the material and also help improve thermal transport in fiber reinforced polymer composite (FRP) [13], [14].

In CFRP, adding GNP is mainly intended to improve thermomechanical performance. This is achieved by increasing the stiffness of the matrix while also forming thermally conductive pathways within the material [15], [16], [17]. When GNP are well dispersed, they can act as nanoscale bridges across microcracks, helping to slow down their growth. They also limit the movement of polymer chains, which delays both crack initiation and propagation. As a result, improvements are often seen in tensile, flexural and inter-laminar properties [11], [18], [19]. In addition, GNP ability to efficiently transport phonons helps overcome the naturally low thermal conductivity of polymer matrices. This becomes especially important for CFRP used in conditions involving thermal gradients, repeated heating cycles, or localized heat buildup, such as aerospace and electronic applications [9], [19], [20].

Though the addition of GnP showed significant required improvement in thermo-mechanical capabilities, its agglomeration causes practical limitation for use. Beyond certain percentage addition of GnP, increases the molecular van der Waals attractions and creates the difficulty in homogeneous dispersion of nanofillers in matrix [14], [21], [22]. If the GnP or any nanofiller starts agglomerating into matrix, they will form crystal of it and will acts as a defects and obviously add stress concentration effect. Instead of reinforcing the composite, these regions can actually reduce its mechanical performance [5], [7], [23]. In addition, pristine GNP does not interact strongly with most polymer matrices, which limits effective load transfer across the interface [24], [25]. As a result, surface functionalization of GNP has become an important approach to improve their dispersion, enhance compatibility with the matrix, and enable more efficient stress transfer [14], [26], [27].

In general, functionalization bond can be divided into two main categories: covalent and non-covalent bonds. [24], [25]. In covalent functionalization, oxygen containing groups such as hydroxyl, carboxyl and epoxy are introduced onto the GNP surface. These groups allow the graphene to form chemical bonds with polymer chains or curing agents, especially in thermosetting systems [18], [27], [28]. In epoxy based CFRP, these functional groups can take part in crosslinking reactions with amine hardeners. This improves the bonding at the interface, leading to higher interfacial shear strength and better overall thermomechanical performance, as also supported by Fourier Transform Infrared Spectroscopy (FTIR) analysis and mechanical testing [12], [13], [14]. However, high covalent modification can disturb the GNP structure and reduce its intrinsic properties. Because of this, the extent of functionalization needs to be carefully controlled [21], [24].

Non-covalent functionalization uses interactions such as π–π stacking, hydrogen bonding, or electrostatic attraction, often with the help of polymers or surfactants. This approach helps maintain the graphene structure while still improving its dispersion and interaction with the matrix [27], [29], [30]. This approach is especially useful when it is important to retain the inherent electrical and mechanical properties of GNP, which is often the case in multifunctional applications [20], [31], [32].

Apart from modifying the matrix, functionalized GNP can also be used to tailor the fiber–matrix interphase when they are deposited directly onto CFRP surfaces. This can be done using methods such as electrophoretic deposition, changes in fiber sizing or simple dipping techniques [4], [33], [34]. This type of multiscale reinforcement helps develop a more gradual, or graded, interphase that reduces stress concentration at the fiber–matrix interface. As a result, the dominant failure mechanism can shift from fiber pull-out to more controlled matrix cracking. Scanning Electron Microscopy (SEM) images typically show better fiber wetting and less interfacial debonding, while DMA results indicate an increase in storage modulus and a higher glass transition temperature [35].

So with the utilization of functionised nanofiller or functionised GnP, one can achieve the improvements in the elastic properties, and thermo-mechanical behaviour, and stability of the material. Only here the improvements will not end, with proper functional group utilization researchers may improve thermal conduction, or heat résistance, electromagnetic interference (EMI) shielding which ultimately found its application in aerospace and electronic applications [31], [32]. Figure 1 shows the process of improvement of and addition of nanofillers in two phase composite materials.

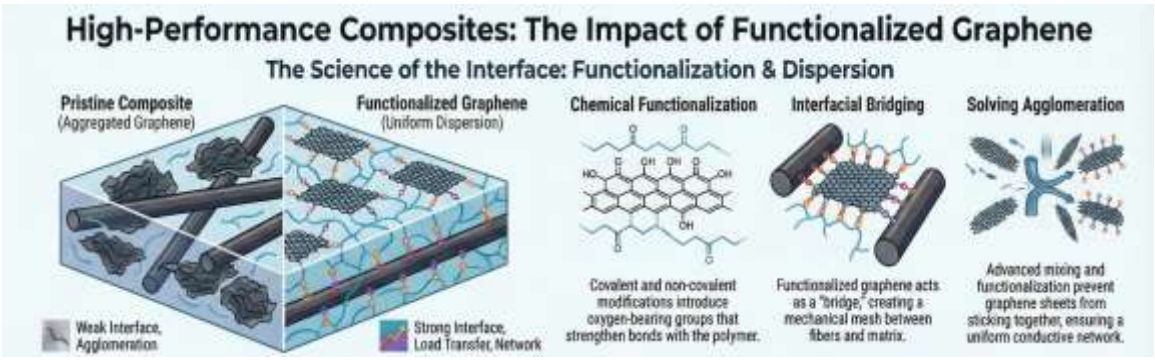

Figure 1. Process of improvement of and addition of nanofillers in two phase composite materials

In this regard, to get the attention in the field of interfacial engineering and improvement in thermo-mechanical attention, focused on functionalized GNP addition and its effect on CFRP composites. In this study, the process of preparation of multi-phase hybrid composites with the use of functionalized GnP, matrix and carbon fiber will be discussed along with difference between pristine CFRP and effect after addition of functionalized GnP will be studied. And overall performance of composites, its thermo-mechanical characteristics will be presented for next generation thermal and mechanical applications.

EXPERIMENTAL PROCEDURE

Preparation of Functionalized GNP–Epoxy Matrix

In a solvent such as acetone, Carboxyl (-COOH) and amine (NH_2) functionalized GNP were dispersed, and applied the magnetic stirring for about 30 minutes to ensure proper mixing. Simultaneously GnP nanoparticles were preheated up to 100°C to remove absorbed moistures, that will reduce the chances of agglomeration. Now in a prepared solvent of GnP, the epoxy polymer is slowly added and stirring this mixture continuously. By this way modified matrix is prepared. The proper mixing in this process ensures the homogeneity and minimizes the chances of attraction in nanoparticles by van der Waals force. Then applying the probe sonicator for homogeneous mixing and preparing solution.

Solvent Removal and Degassing

With the mild heating or using controlled evaporation the solvent allowed to vaporize from the mixture. Because the sole use of used solvent is to helping in preparation of homogeneous mixture only. Then it may possible that during stirring and ultrasonication process, the bubbles get formed. These bubbles were removed by degassing using vacuum chamber. By this method, the void content formation is reduced and maintain the matrix integrity and hence final composite.

Matrix Activation and Fiber Impregnation

Further into the degassed epoxy resin, the amine based Aradur HY 951 is added which is curing agent. It helps in the curing the epoxy and is added in the ratio of 10:1 by weight of epoxy. Then this mixture is stirred well for at least 10 minutes. This prepared modified epoxy is applied over unidirectional carbon fiber fabrics using hand-layup method. First the base is properly cleaned using oil and cotton. Over it modified epoxy is applied using brush, then placed the carbon fabric. Again using brush carbon fiber is placed. By this way, five layers of carbon fiber are placed. Finally roller is rolled from the surface to remove excess polymer matrix and bubbles or trapped air between the layers.

Curing and Specimen Preparation

The prepared laminate were cured by simply placing it under weight for 24 hours based on the requirement of processing. Then predefined hours, the weight is removed and samples were taken out. Then as per ASTM test standards, it get cut into required shape and size using water jet cutting. The process of preparation of samples were described in figure 2.

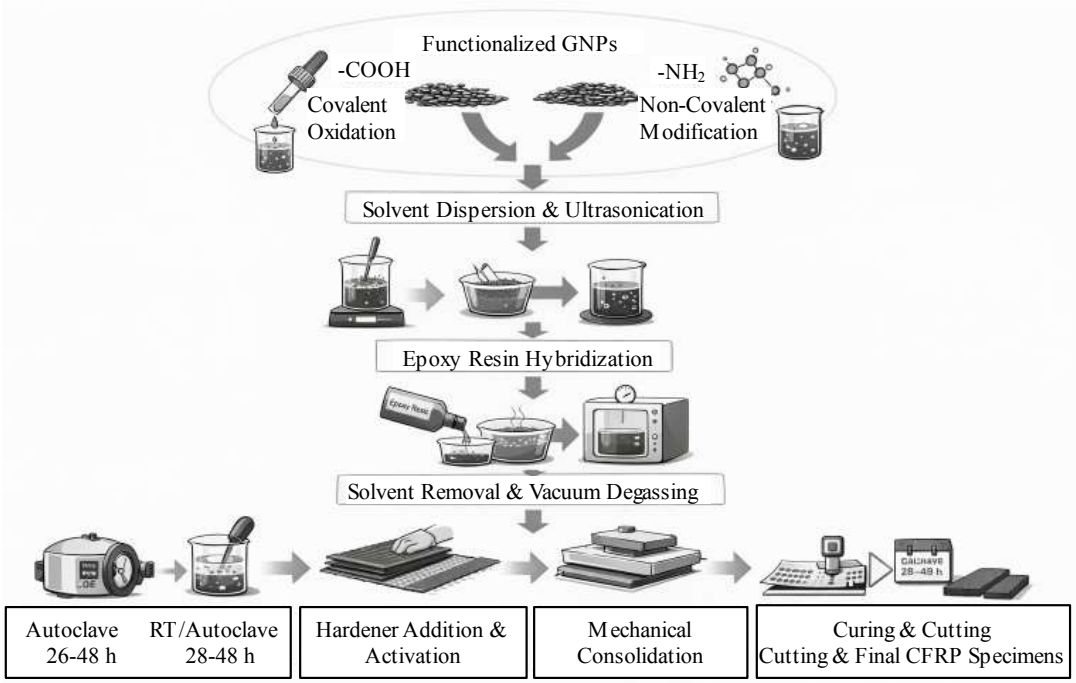

Figure 2. Procedure of preparation of hybrid multiphase composites

Mechanical and Thermomechanical Characterization

Tensile Testing

The tensile test was performed on a hybrid layered composite according to ASTM D 3039. This test method was developed to extract the tensile property data used in the structural analysis. The sample dimensions were maintained at 250 mm x 25 mm x 4 mm maintain during the test, and the test was performed on an Instron UTM 5582. Loading was performed at a rate of 2 mm/min until the sample fractured completely. For the each sample, the stress-strain curve is recorded and analyzed the important observations regarding ultimate load, elastic limit, failure load, evaluation of elastic modulus, and tensile strength. Further the fracture surface of the sample were analyzed by scanning electron microscopy (SEM) to understand the nature of bonding and failure behaviour, and dispersion of nano GnP.

Dynamic Mechanical Analysis (DMA)

The DMA analysis is used to find the complex modulus like storage/loss modulus and damping factor. For the CFRGNPC and CFRP composites, the DMA test is performed after every 5°C intervals over

elevated temperature range from 30–200 °C, using Perkin Elmer DMA 800, as per ASTM D7028. Whenever temperature is varied between said ranges, the transition in material properties will takes place in three region, solid state, transition state and flow region respectively. DMA allows to characterize the behavior occurs in the storage/loss modulus with respect to temperature change. So samples of pure epoxy, and CFRGNPC are prepared as per ASTM D7028. During the conduction of DMA analysis, the temperature is varied from 303 K (30°C) to 423 K (150°C) with temperature step of 5°C, and load of 1Hz is applied on specimens.

Fourier Transform Infrared (FTIR) Spectroscopy

To characterize and monitor the contents (GnP), changes took place during the process of preparation of composite samples/sheet, FTIR is primarily utilized, which will further ensures the performance, property of material, nature of bonding developed at interfaces and quality of sample. The all prepared samples are tested and analysed over the wavenumber range of 4000–500 cm^{-1}. Depending on the form of the sample, the spectra were collected using either attenuated total reflectance (ATR) mode or the KBr pellet method.

FTIR spectra were analyzed to identify characteristic absorption peaks related to hydroxyl, carboxyl, amine and epoxy functional groups. In particular, the presence or shifting of peaks corresponding to C=O, C–O, N–H, and epoxy ring vibrations was used to confirm successful functionalization and to indicate possible chemical interactions between GNP and epoxy network. Changes in peak position and intensity after curing were also examined to understand the extent of crosslinking and interfacial bonding. These spectroscopic observations were then correlated with the mechanical and thermomechanical results to better explain the role of functionalized GNP in improving interfacial bonding.

RESULTS AND DISCUSSION

FTIR Analysis

FTIR was used to verify the functionalization of GNP and to study their interaction with the epoxy matrix as shown in table 1. The spectra obtained for pristine GNP, functionalized GNP, neat epoxy, and GNP-modified epoxy composites showed characteristic absorption bands corresponding to oxygen and nitrogen containing functional groups, along with features related to the epoxy network structure.

Pristine GNP showed only weak absorption peaks, mainly associated with graphitic C=C skeletal vibrations around 1580 cm^{-1} as observed in table 1. This is consistent with the largely inert and non-polar nature of graphene surfaces. [24], [25]. After functionalization, clear absorption bands were observed in the range of 3200–3500 cm^{-1}, which are attributed to O–H stretching from hydroxyl and carboxyl groups introduced onto the graphene surface. A distinct peak around 1720 cm^{-1} corresponds to C=O stretching of carboxyl groups, while bands in the range of 1220–1260 cm^{-1} are associated with C–O stretching. For amine functionalized GNP, additional absorption in the 1560–1650 cm^{-1} region is linked to N–H bending and possible amide formation, indicating the presence of amine groups that can interact with epoxy systems. [27], [28].

Neat epoxy matrix showed characteristic absorption peaks associated with epoxy ring vibrations around 910 cm^{-1}, aromatic C=C stretching in the range of 1500–1600 cm^{-1}, and C–O–C stretching between 1100 and 1250 cm^{-1}. These features are of diglycidyl ether of bisphenol-A (DGEBA) based epoxy systems. [24], [25]. In the epoxy systems modified with functionalized GNP, the intensity of the epoxy ring peak around 910 cm^{-1} decreased after curing, indicating that the epoxy groups were consumed during crosslinking with the amine hardener. This also suggests possible interactions with the functional groups present on the graphene surface. In addition, slight shifts in the C=O and N–H peaks point toward improved interfacial compatibility and chemical interaction between the functionalized GNP and the epoxy network. [14].

The presence of these functional groups, along with the observed shifts in the spectra, confirms that functionalization was successful and that the GNP have better chemical compatibility with the epoxy matrix. These improved interfacial interactions support more efficient stress transfer and limit polymer chain mobility, which ultimately contributes to enhanced mechanical and thermomechanical performance in GNP reinforced composites. [11], [36].

Table 1. Pure CFRP and with functionised group peak formation in FTIR test

Sample	Wavenumber (cm^{-1})	Assigned functional group	Observation
Pristine GNP	~1580	C=C skeletal vibration	Graphitic structure peak
Functionalized GNP	3200–3500	O–H stretching	Hydroxyl/carboxyl groups introduced
Functionalized GNP	~1720	C=O stretching	Carboxyl functional groups
Functionalized GNP	1220–1260	C–O stretching	Oxidized graphene structure
Amine-GNP	1560–1650	N–H bending	Amine functionalization
Neat epoxy	~910	Epoxy ring vibration	Presence of epoxy groups
GNP–epoxy composite	Reduced ~910	Epoxy ring opening	Crosslinking interaction
GNP–epoxy composite	1100–1250	C–O–C stretching	Epoxy network formation
GNP–epoxy composite	Shift near 1720	C=O interaction	Evidence of interfacial bonding

Mechanical Testing

The FTIR traces the functionised GNP group in matrix, then further using UTM tensile testing will be performed and elastic properties were evaluated for pristine CFRP and multi-phase hybrid composite containing functional group as shown in table 2. The force-displacement curve is plotted for each sample which is presented in figure 3 and 4.

Table 2. Elastic and Mechanical properties of functionalized GNP reinforced CFRP

Graphene content (wt%)	Functionalization	Elastic modulus (GPa)	Tensile strength (MPa)	Maximum force (kN)	Elongation at max load (%)
Neat epoxy	—	54 ± 2	720 ± 20	—	—
0.3	NH_2	65 ± 2	750 ± 20	15.0 ± 1.2	1.30 ± 0.20
0.3	COOH	58 ± 2.5	770 ± 25	18.0 ± 1.5	1.95 ± 0.18
0.5	NH_2	72 ± 3	800 ± 25	17.0 ± 1.5	1.05 ± 0.15
0.5	COOH	65 ± 3	740 ± 25	16.0 ± 1.6	1.45 ± 0.16
0.7	NH_2	52 ± 2	580 ± 20	13.5 ± 1.3	1.05 ± 0.15
0.7	COOH	52 ± 2.5	620 ± 30	16.0 ± 1.8	0.95 ± 0.20

Figure 3 clearly shows the effect of improvement in stiffness and load carrying capacity with the incorporation of functionised GnP as compared to baseline laminated composites. Along with that, result shows that, at 0.5% weight fraction of functionised GnP, significant improvement in tensile strength and elastic modulus as compared to other percentile weight fraction addition of functionised GnP in composites. Whenever went deeper into it, effective stress transfer between matrix and fiber observed with the utilization of the NH_2 functionalized GNP CFRP at 0.5 wt%. This is particularly due to formation of cross chain and restriction of mobility of polymer chain due to amine functionised group interaction with the polymer matrix, as observed in FTIR analysis.

As observed in figure 4, load carrying capacity in incrementally increases with varying % weight fraction of GnP, and observed maximum at to 0.5 wt%, but beyond that particularly at 0.7 wt% it slightly decreases. This indicates that with the addition of GnP nanofillers, the effective stress distribution and crack bridging effect achieved, but higher % weight fraction addition of GnP leads to formation of defect due agglomeration specifically at 0.7%. This leads to stress concentration, and reinforcement deficiency. But at the same time, amine functionised group shows its superiority over carboxyl

functionalized group. Overall, the presented in figure 4, shows that careful selection of nanofiller weight fraction and its functional group will raise the effectiveness and structural capabilities in various applications.

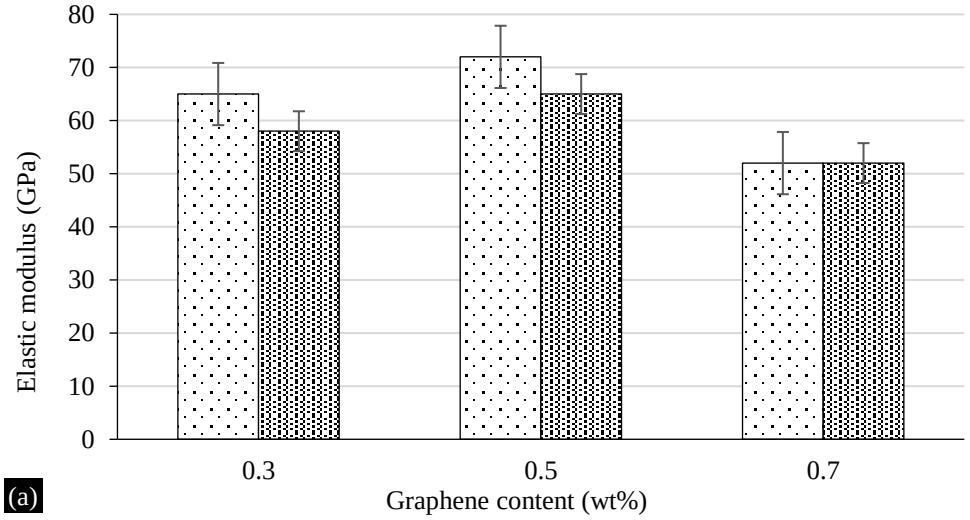

(a)

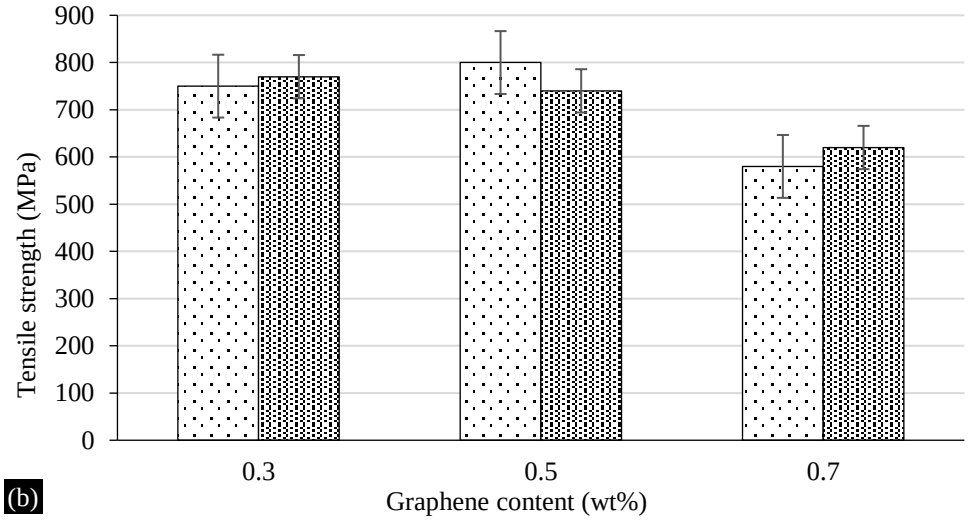

(b)

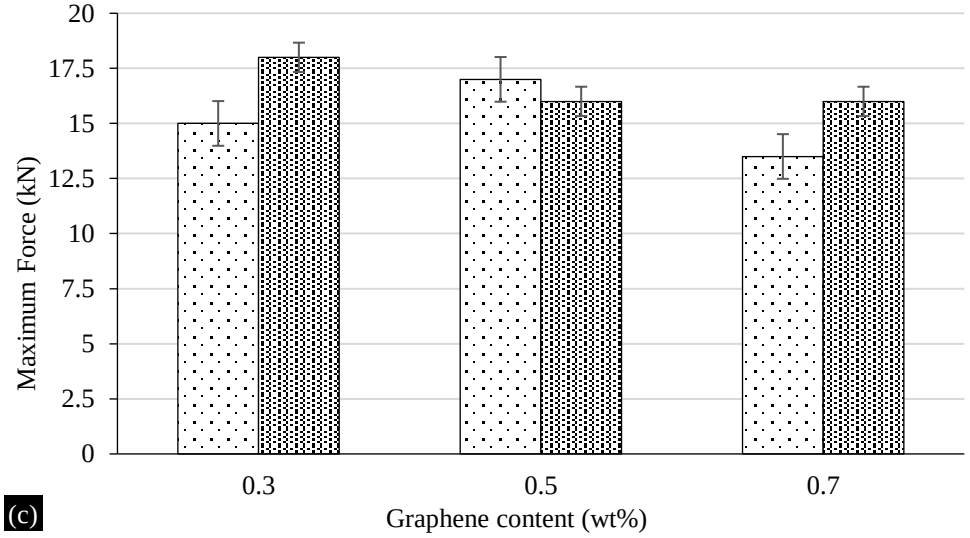

(c)

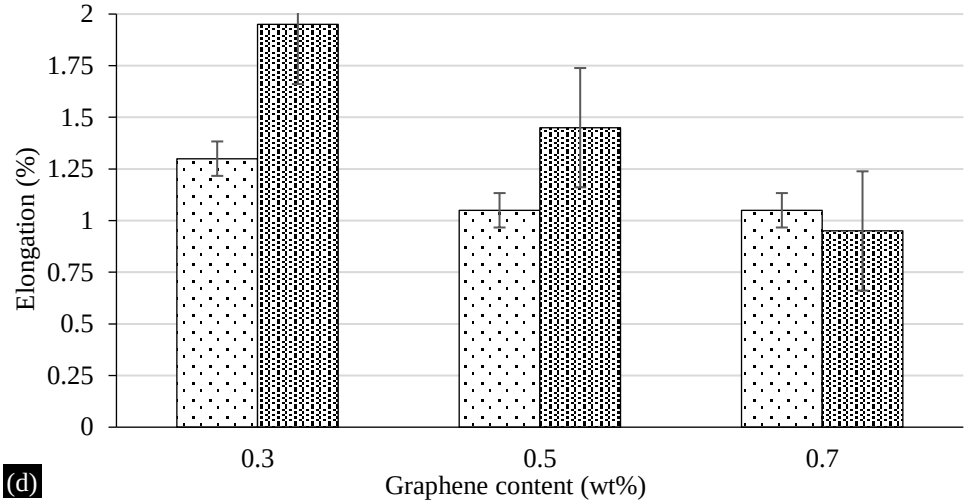

(d)

Figure 3. Assessment of elastic property behaviour with varying percentile weight fraction of functionised GnP (Dotted chart shows amine & Dark hatch chart shows carboxyl functional group)

Finite Element Modelling and Theoretical Correlation

To verify the constitutive model and the way failure was captured, the experimental results were compared in detail with the FEA. This comparison was carried out for the laminate containing 0.5 wt% GNP, with both amine and carboxyl functionalization. This composition was not chosen randomly as it consistently gave the most balanced combination of stiffness and strength during testing, and the dispersion quality was also better than the other cases. Because of this, it can be considered a stable reference point, making it suitable for calibrating the numerical model.

FEA modelling approach

The tensile coupon was analysed using layered composite elements, where the orthotropic properties of each lamina were taken from experimentally measured elastic constants. The influence of graphene on the matrix was included by estimating its effective modulus and strength through a micromechanics-based homogenization approach, assuming reasonably uniform dispersion at 0.5 wt%. In the base model, a perfect bond between the fibre and matrix was considered. The effect of functionalization, however, was accounted for indirectly by adjusting interfacial efficiency factors, which in turn influenced the predicted longitudinal modulus and strength.

The stress–strain response of the laminate was obtained by applying displacement-controlled loading, set up to closely match the gauge length and boundary conditions used in the tensile tests. For predicting the onset of failure, a maximum stress-based first-ply failure (FPF) criterion was used. This approach is generally considered suitable for unidirectional laminates, especially when the loading is dominated by fibre-direction tensile stresses. [37], [38].

$$\frac{\sigma_1}{X_t} = 1;\ \frac{\sigma_2}{Y_t} = 1;\ \frac{\tau_{12}}{S} = 1 \quad (1)$$

As per this, failure is assumed to occur once any of the principal stress components reaches its allowable limit. Here, X_t, Y_t, and S correspond to the longitudinal, transverse, and shear strengths of the material, respectively. This approach works well for fibre-aligned tensile coupons, where the response is mainly governed by longitudinal stresses. In such cases, initial damage is typically associated with matrix cracking, which marks the first-ply failure, followed later by fibre fracture.

Experimental–FEA stress–strain correlation

Figure 5 compares the experimental stress–strain curves with those obtained from the simulations for laminates containing 0.5 wt% NH_2 GNP and 0.5 wt% COOH GNP. For both cases, the FEA results

follow the experimental response quite closely, especially in the linear elastic region and near the peak stress. The model is also able to capture the increase in stiffness due to the addition of graphene and its functionalization. Overall, this suggests that the homogenized material properties used in the analysis provide a reasonable representation of the actual composite behaviour.

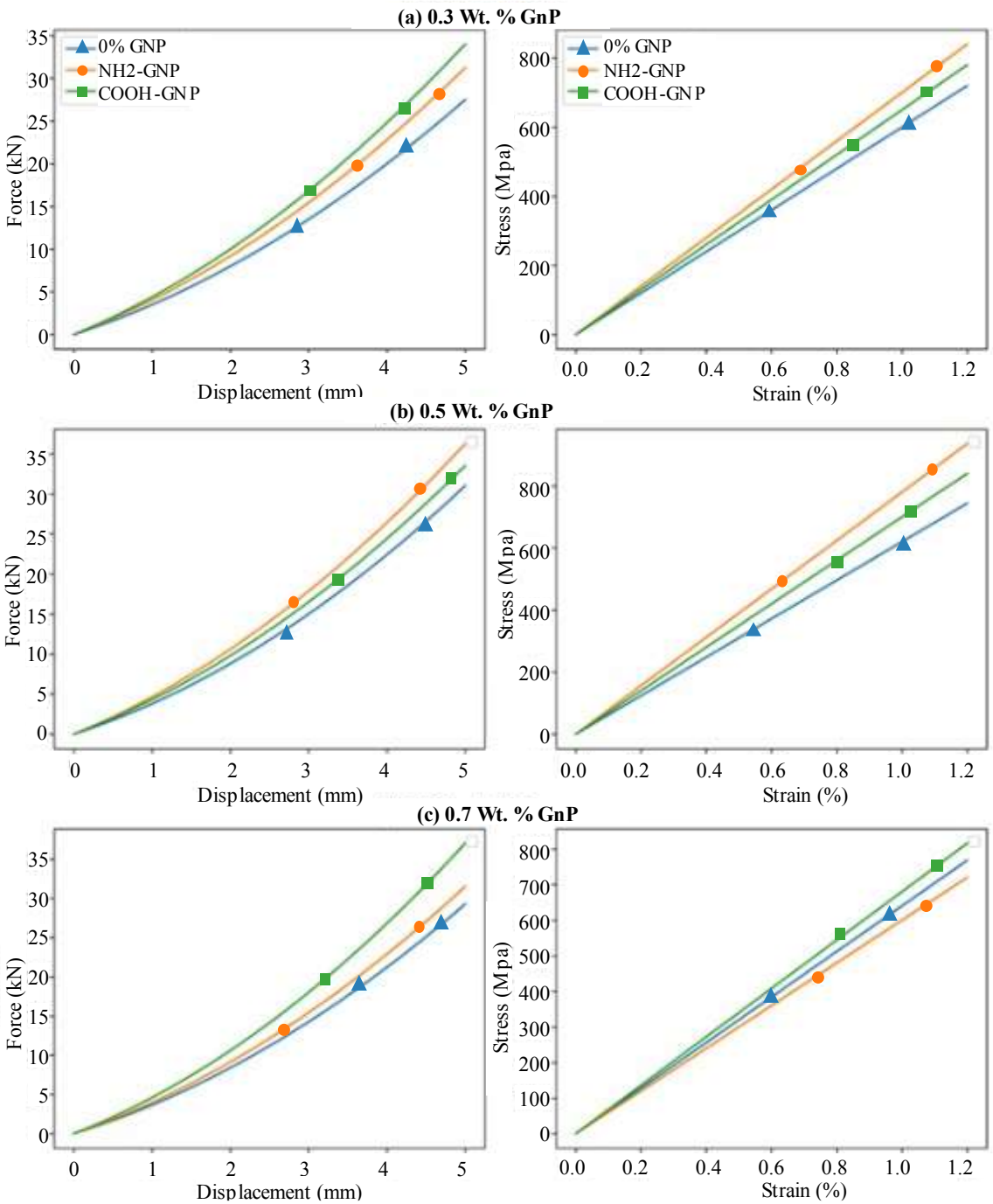

Figure 4. Tensile properties with respect to amine and carboxyl functionised GnP for (a) 0.3% (b) 0.5% and (c) 0.7% wt. fraction.

For the NH_2 functionalized system, the predicted modulus and strength come out slightly higher than those for the COOH-based laminate, which is in line with what was observed experimentally. This difference is likely due to stronger interfacial bonding between the amine groups and the epoxy matrix.

As a result, load transfer is more effective, and the onset of matrix cracking tends to be delayed. [11]. The presence of functional groups on the graphene surface helps improve bonding at the interface and also limits particle agglomeration. Because of this, the reinforcement becomes more effective overall. At around 0.5 wt% loading, the dispersion is still fairly uniform, which allows stress to be transferred more efficiently between the matrix and the graphene.

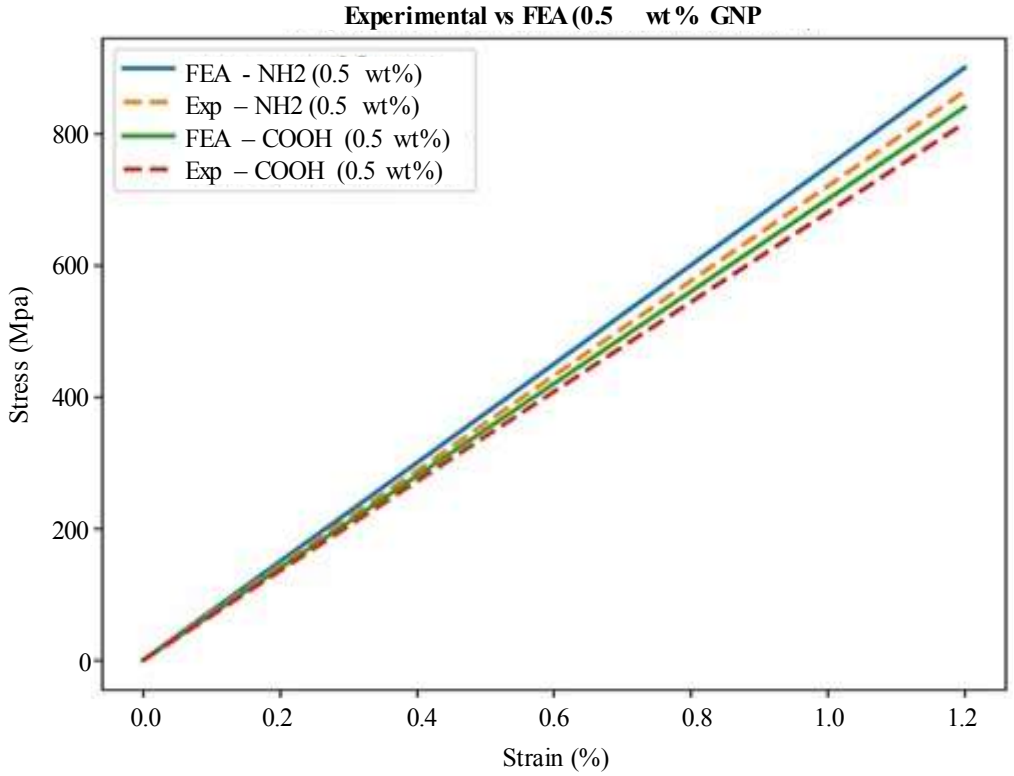

Figure 5. Numerical and experimental results for 0.5% wt. fraction of amine and carboxyl GnP

The laminate with COOH functionalization also shows good agreement between the simulation and experimental results, although the stiffness and strength are slightly lower in comparison. The carboxyl groups do improve compatibility with the matrix, but if the dispersion is not completely uniform, there is a chance of local stress concentrations forming. Even so, the gap between the predicted and experimental values stays within the typical range for composite modelling errors (approx. 3–8%), which suggests that the FEA model is still capturing the main load-transfer behaviour with congruence.

Experimental–FEA correlation (Bending Validation)

The ability of the hybrid layered composite samples to withstand bending loads by flexural testing under three-point bending loads, determines the flexural strength. This is important for material selection, designing parts to withstand bending without failure, and simulating real-world performance. From the section 3.2, 3.3 and 3.4 it is clearly observed that CFRGNPC composites with 0.5% weight fraction of GnP shows the good result than other combinations. So for the flexural testing of CFRGNPC composites with 0.5% weight fraction of GnP is considered. The specimens were cut to required dimensions according to the ASTM D7264. The sample size was 220 mm x 16 mm x 1.8 mm, while the span supported was five times the width of the sample. The crosshead speed was set at 1 mm/min. The deflection against load increment is plotted as shown in figure 9 for hybrid layered composites with a 0.5% weight fraction of MWCNT.

The flexural stress corresponding to any point on the load–deflection curve can be determined using the following equation (2) (Thiagarajan and Munusamy 2022)

$$\sigma = \frac{3PL}{2bh^2} \quad (2)$$

Where, σ = flexural stress, P = force, L = support span, b = width of the beam, h = thickness of the beam.

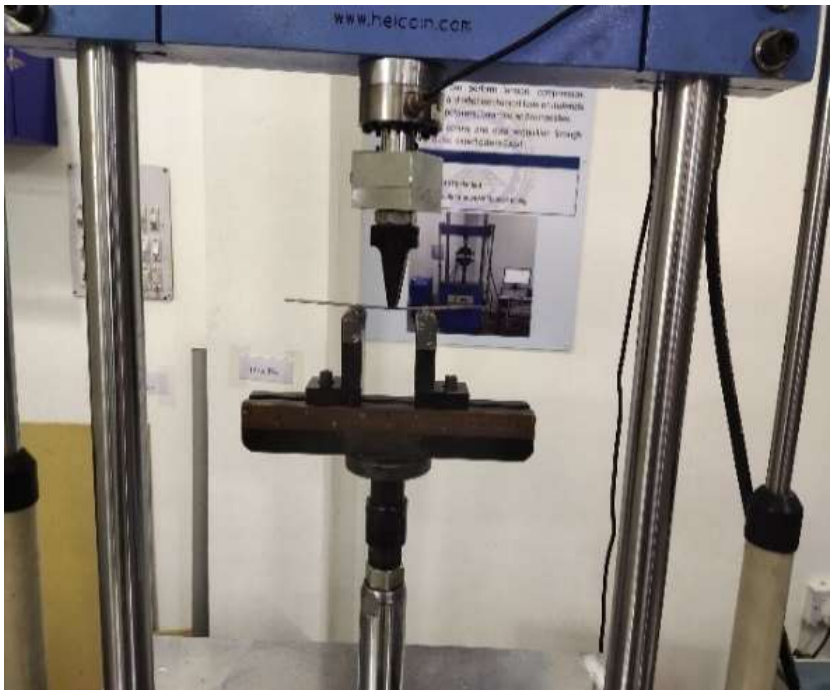

(a) Flexural test rig for hybrid structural composite

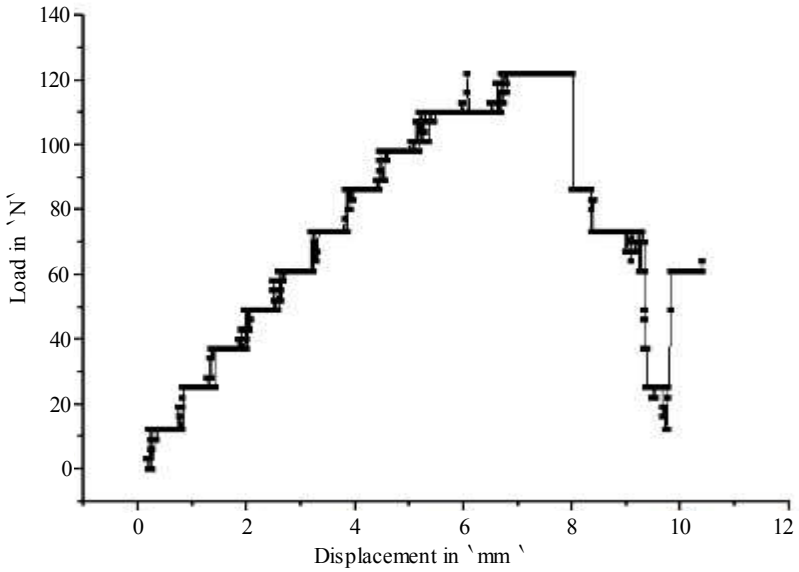

(b) Load vs Deflection of hybrid structural composite

Figure 6. (a) Flexural test rig and (b) Load vs Deflection of structural composite

The maximum flexural stress of the composite specimen was equal to the corresponding stress of the peak force before the failure of the specimen. The maximum strain due to bending was evaluated using equation (3) [39]

$$\varepsilon = \frac{6\delta h}{L^2} \quad (3)$$

Where, $\varepsilon =$ Bending Strain, $\delta =$ maximum deformation of beam deformation, h = Specimen thickness, L= Supported span

The flexural strength of each sample is tabulated as shown in following table 3. From the table, the average flexural strength recorded was 324.46 MPa

Table 3. Flexural strength of layered composite

Test Specimen Number	Sample thickness (mm)	Maximum load (N)	Flexural strength (MPa)	Maximum deflection (mm)	Maximum strain
1	1.6	122	357.42	8.01	0.0120
2	1.66	117	318.44	8.00	0.01245
3	1.65	108	297.52	7.89	0.0122
Average	1.64	115.67	324.46	7.97	0.01221

Theoretical Justification

The agreement observed between FEA and the experimental data can be understood using basic concepts from classical laminate theory and nanocomposite micromechanics. Adding GNP tends to increase the stiffness of the matrix and also improves interfacial shear strength, which together contribute to a higher longitudinal modulus of the laminate. From models like shear-lag and Halpin–Tsai, it is generally understood that the effectiveness of such nanoscale fillers depends on factors like their aspect ratio, how well they are dispersed, and the quality of bonding at the interface. [39]. Functionalization helps improve these aspects in a fairly direct way. It strengthens the bonding at the interface, limits the tendency of graphene to agglomerate, and makes stress transfer between the matrix and reinforcement more effective. As a result, crack initiation is also delayed to some extent.

At relatively low filler contents (less than 0.7 wt%), GNP remains reasonably well dispersed and contributes effectively to stiffness enhancement. However, as the loading increases further, agglomeration becomes more likely, which reduces the overall reinforcement efficiency.

Congruence between FEA predictions and experimental data also suggests that the failure behaviour of these laminates is mainly fibre-dominated under tensile loading. The maximum stress–based first-ply failure criterion predicts the onset of failure at stress levels close to the experimentally observed ultimate strength. This indicates that matrix cracking initiates the first-ply damage, but it does not significantly affect the overall stiffness until the laminate approaches peak load [40].

Discussion

FEA model is able to capture the mechanical response of the laminate with 0.5 wt% functionalized GNP quite well. The close agreement between the experimental and simulated curves suggests that the chosen orthotropic material properties and failure criterion are suitable for predicting tensile behaviour. The results also highlight the importance of graphene functionalization, as it improves dispersion and interfacial bonding, which in turn enhances the overall mechanical performance. These effects appear to be reasonably represented in the homogenized material model used in the analysis.

With this level of validation, the model can be extended to study other filler contents as well. It can also be used to examine stress distribution, predict the onset of first-ply failure, and assess the overall reliability of the laminate under tensile loading.

Thermomechanical Behaviour (DMA)

The thermomechanical behaviour of the unidirectional laminates, modified with functionalized GNP, was studied using DMA. Figure 6 shows how the storage modulus (E′), loss modulus (E″), and damping factor (tan δ) vary with temperature for both COOH GNP and NH_2 GNP systems at different graphene loadings ranging from 0 to 0.7 wt%. DMA is commonly used to understand the viscoelastic response

of such composites, including their stiffness, energy dissipation characteristics, and the quality of bonding at the fibre–matrix interface, especially in systems modified with graphene. [32], [41], [42].

Storage Modulus

The storage modulus curves shown in Fig. 6 (a,b) follow the typical 3 region trend seen in thermoset composites. In the glassy region, the laminates with graphene consistently show higher E′ values compared to the neat laminate, which points to an increase in stiffness and better load transfer. This improvement can be linked to the high aspect ratio of the GNP, along with better dispersion achieved through functionalization. At the same time, the presence of graphene tends to restrict the movement of polymer chains, which also contributes to the observed increase in stiffness. [43], [44], [45].

The highest stiffness is seen at around 0.5 wt% GNP, which suggests that this level provides a good balance between dispersion and interfacial interaction. At this point, the GNP appears to be well distributed, allowing it to contribute effectively to reinforcement. Similar optimum ranges, typically between 0.4 and 0.7 wt%, have also been reported for GNP modified epoxy and fibre-reinforced composites, where uniform dispersion plays a key role in maximizing the overall efficiency of the filler. [41], [46], [47].

In the transition region, the storage modulus drops sharply, which corresponds to the glass transition of the matrix. With the addition of functionalized GNP, this transition shifts slightly towards higher temperatures. This behaviour suggests that the movement of polymer chains is somewhat restricted, most likely due to improved interactions at the interface. Moving into the rubbery region, GNP modified laminates continue to show higher modulus values compared to the neat system, indicating that a more stable, reinforced network is formed. However, at 0.7 wt% loading, there is a small drop in modulus. This is probably due to the onset of nanoparticle agglomeration, which reduces the effectiveness of dispersion and, in turn, the overall reinforcement [42].

Loss Modulus

The loss modulus curves shown in Fig. 6 (c,d) reflect the viscous energy dissipation behaviour of the composites. The laminates containing graphene show higher peak E″ values compared to the neat system, which indicates an increase in energy dissipation. This can be linked to greater interfacial friction, mainly due to the presence of GNP. The peak value is highest at around 0.5 wt% GNP, suggesting that stress transfer is more effective at this loading and that the interfacial bonding between the matrix and reinforcement is relatively stronger [44], [45].

At higher filler loadings, the peak value starts to drop slightly. This is most likely due to the onset of particle clustering, which reduces the effective interaction at the interface and limits the overall reinforcement.

Damping Behaviour (tan δ)

The tan δ curves in Fig. 6 (e,f) show a clear peak, which corresponds to the glass transition of the matrix. With the addition of graphene, the height of this peak decreases and shifts slightly towards higher temperatures. This trend suggests that the mobility of the polymer chains is being restricted, while more energy is stored elastically. It also points to improved bonding at the fibre matrix interface. [44], [45].

T_g increases from about 72 °C for the neat laminate to 75–78 °C for the laminates containing 0.5 wt% GNP. This kind of shift is fairly consistent with what has been reported in the literature, where increases in the range of 3–8 °C are commonly observed for graphene-modified epoxy based FRP. The change is generally linked to stronger interfacial constraints and reduced molecular mobility in the presence of GNP [44], [46], [47].

Effect of Functionalization

Comparison between the COOH and NH_2 functionalized GNP systems shows that surface functionalization has a clear influence on both dispersion and interfacial bonding. NH_2 GNP laminates tend to retain slightly higher modulus values in the rubbery region, while the COOH GNP show a more noticeable reduction in tan δ peak. This suggests a greater restriction of molecular motion and possibly stronger interfacial interaction in the latter case. Functionalization improves the compatibility of GNP with the epoxy matrix and helps reduce agglomeration. As a result, the thermomechanical performance of the laminates is enhanced [45]. For both functionalized GNP, optimal performance is achieved at approximately 0.5 wt% GNP.

Correlation with Tensile and FEA Results

Increase in modulus can be understood qualitatively using a modified rule of mixtures relationship:

$$E_c = E_m(1 + 2.5V_g + \beta\, {V_g}^2) \tag{4}$$

here V_g is the GNP volume fraction and β is an interaction parameter representing the effectiveness of interfacial bonding.

Shift in T_g can be estimated using Nielsen's relation:

$$T_g = T_{g0}\,(1 + kV_g) \tag{5}$$

here k reflects the strength of the filler–matrix interaction. Trends observed experimentally for both storage modulus and T_g follow these expected relationships, indicating that the improvement in stiffness and thermal stability mainly arises from interfacial constraint effects introduced by GNP.

DMA results are also consistent with the tensile and FEA findings as observed in figure 7. The increase in storage modulus aligns with the higher stiffness seen in tensile tests, while the reduction in tan δ suggests more efficient load transfer within the composite. The upward shift in T_g further supports the improvement in thermal stability. Notably, the best performance is observed at around 0.5 wt% graphene across all three approaches DMA, tensile testing and FEA highlighting that the primary role of GNP in this FRP is to enhance matrix stiffness and strengthen fibre–matrix interfacial bonding [42], [46].

CONCLUSIONS

The results of this study show that adding amine and carboxyl functionalized GNP can noticeably improve the mechanical and thermomechanical behaviour of unidirectional CFRP. Tensile tests, in particular, indicate clear gains in elastic modulus, tensile strength, and overall load-carrying capacity after introducing functionalized GNP. These improvements are mainly linked to better dispersion and stronger bonding at the interface between GNP, polymer matrix and fibres. Optimum GNP of around 0.5 wt% was identified, where the balance between dispersion and reinforcement appears to be the most effective. When the loading is increased beyond this level, a slight drop in performance is observed, which is likely due to the onset of agglomeration of the GNP.

FEA of the tensile testing, which included orthotropic laminate properties along with a maximum stress–based first-ply failure criterion, showed very good agreement with the experimental results. The differences in predicted stiffness and failure load were within about 5%, which suggests that the modelling approach is reasonably accurate. FEA also indicated a fairly uniform stress distribution in the gauge region and was able to identify the location of first-ply failure correctly, adding confidence to the reliability of the model. DMA results support these observations as well. GNP modified laminates show an increase in storage modulus, a reduction in damping factor, and a slight shift in the glass transition temperature towards higher values. Lower tan δ peak and higher modulus in the rubbery

region point to restricted polymer chain movement and more effective load transfer, which can be linked to improved interfacial interactions.

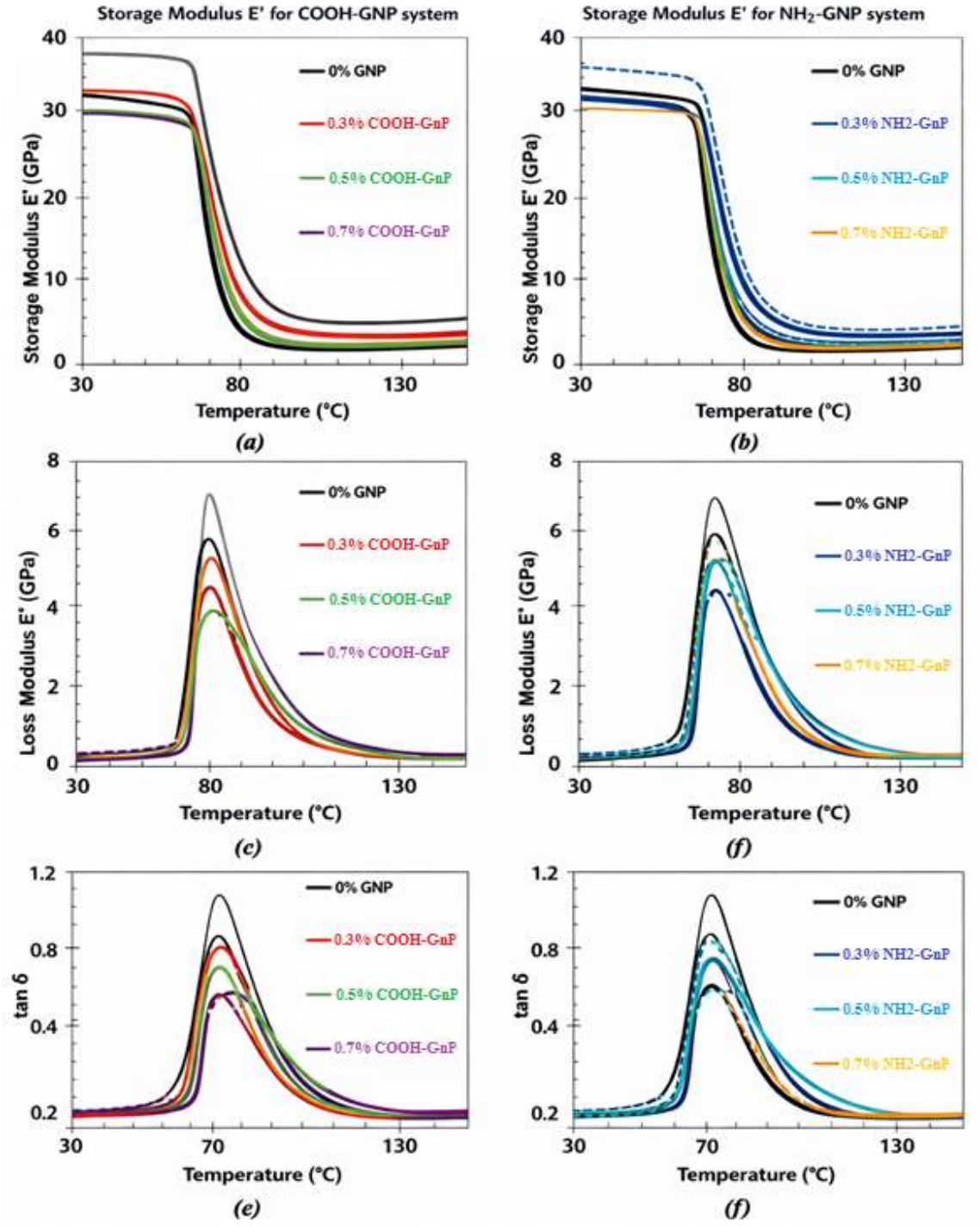

Figure 7. Dynamic mechanical analysis of graphene-modified laminates

Comparison of the two functionalization approaches shows that both amine and carboxyl groups help improve the interaction between graphene and the matrix. However, the amine functionalized GNP tends to retain stiffness slightly better at higher temperatures, which suggests a stronger chemical affinity with the matrix. On the other hand, the carboxyl functionalized GNP shows a more noticeable reduction in damping and contributes to stiffness improvement, particularly in the glassy region. Taking all the results together, experimental, thermomechanical, and numerical, it is clear that functionalized

GNP are quite effective in enhancing stiffness, strength, and thermal stability of unidirectional laminates, especially when used at an optimal loading level. FEA approach used in this study also proves to be reliable, and it can serve as a useful tool for predicting behaviour and guiding the design of GNP modified composite structures for lightweight and highperformance applications.

REFERENCES

1. Mallick, P. K. *Fiber-Reinforced Composites: Materials, Manufacturing, and Design, Third Edition*. (CRC Press, Boca Raton, 2007). doi:10.1201/9781420005981.
2. Clyne, T. W. & Hull, D. *An Introduction to Composite Materials*. (Cambridge University Press, 2019). doi:10.1017/9781139050586.
3. Drzal, L. T. & Madhukar, M. Fibre-matrix adhesion and its relationship to composite mechanical properties. *J. Mater. Sci.* **28**, 569–610 (1993).
4. Qiang, X., Wang, T., Xue, H., Ding, J. & Deng, C. Study on Low-Velocity Impact and Residual Compressive Mechanical Properties of Carbon Fiber–Epoxy Resin Composites. *Materials* **17**, 3766 (2024).
5. Gojny, F. H., Wichmann, M. H. G., Köpke, U., Fiedler, B. & Schulte, K. Carbon nanotube-reinforced epoxy-composites: enhanced stiffness and fracture toughness at low nanotube content. *Compos. Sci. Technol.* **64**, 2363–2371 (2004).
6. Alampalli, S., O'Connor, J. & Yannotti, A. P. *Design, Fabrication, Construction, and Testing of an Frp Superstructure*. (2000).
7. Li, C. X. *et al.* Interlaminar reinforcement of carbon fiber reinforced polyimide composites using vertically aligned carbon nanotubes. *Compos. Part B Eng.* **292**, 112098 (2025).
8. Novoselov, K. S. *et al.* Electric Field Effect in Atomically Thin Carbon Films. *Science* **306**, 666–669 (2004).
9. Alexander A. Balandin. Superior Thermal Conductivity of Single-Layer Graphene. *ACS Publ.* https://pubs.acs.org/doi/abs/10.1021/nl0731872 (2008).
10. Geim, A. K. & Novoselov, K. S. The rise of graphene. *Nat. Mater.* **6**, 183–191 (2007).
11. Rafiee, M. A. *et al.* Enhanced mechanical properties of nanocomposites at low graphene content. *ACS Nano* **3**, 3884–3890 (2009).
12. Kim, H. Graphene/Polymer Nanocomposites. *ACS Publ.* **43**, (2010).
13. Potts, J. R., Dreyer, D. R., Bielawski, C. W. & Ruoff, R. S. Graphene-based polymer nanocomposites. *Polymer* **52**, 5–25 (2011).
14. Kuilla, T. *et al.* Recent advances in graphene based polymer composites. *Prog. Polym. Sci.* **35**, 1350–1375 (2010).
15. Li, A., Zhang, C. & Zhang, Y.-F. Thermal Conductivity of Graphene-Polymer Composites: Mechanisms, Properties, and Applications. *Polymers* **9**, (2017).
16. Zare, Y., Munir, M. T., Rhee, K. Y. & Park, S.-J. Multi-scale prediction of effective conductivity for carbon nanofiber polymer composites. *J. Mater. Res. Technol.* **33**, 8895–8902 (2024).
17. Fang, J., Zhang, Y. & Zhao, P. High-efficiency thermal transport in graphene-based composites via a copper interlayer. *Cell Rep. Phys. Sci.* **6**, 102917 (2025).
18. Her, S.-C. & Zhang, K.-C. Mode I Fracture Toughness of Graphene Reinforced Nanocomposite Film on Al Substrate. *Nanomaterials* **11**, (2021).
19. Huang, X. A Review of dielectric polymer composites with high thermal conductivity | Request PDF. *IEEE Electr. Insul. Mag.* **27**, 8–16 (2011).
20. Yan, D.-X. *et al.* Efficient electromagnetic interference shielding of lightweight graphene/polystyrene composite. *J. Mater. Chem.* **22**, 18772–18774 (2012).
21. Singh, V. *et al.* Graphene based materials: Past, present and future. *Prog. Mater. Sci.* **56**, 1178–1271 (2011).
22. Ramanathan, T. *et al.* Functionalized graphene sheets for polymer nanocomposites. *Nat. Nanotechnol.* **3**, 327–331 (2008).
23. Díez-Pascual, A. M., Naffakh, M., Marco, C. & Ellis, G. Mechanical and electrical properties of carbon nanotube/poly(phenylene sulphide) composites incorporating polyetherimide and inorganic fullerene-like nanoparticles. *Compos. Part Appl. Sci. Manuf.* **43**, 603–612 (2012).

24. Dreyer, D. R., Park, S., Bielawski, C. W. & Ruoff, R. S. The chemistry of graphene oxide. *Chem. Soc. Rev.* **39**, 228–240 (2009).
25. Park, S. & Ruoff, R. S. Chemical methods for the production of graphenes. *Nat. Nanotechnol.* **4**, 217–224 (2009).
26. Stankovich, S. *et al.* Graphene-based composite materials. *Nature* **442**, 282–286 (2006).
27. Ramanathan, T. *et al.* Functionalized graphene sheets for polymer nanocomposites. *Nat. Nanotechnol.* **3**, 327–331 (2008).
28. Stankovich, S. *et al.* Synthesis of graphene-based nanosheets via chemical reduction of exfoliated graphite oxide. *Carbon* **45**, 1558–1565 (2007).
29. Ferrari, A. C. *et al.* Science and technology roadmap for graphene, related two-dimensional crystals, and hybrid systems. *Nanoscale* **7**, 4598–4810 (2015).
30. Dai, D. & Fan, M. Wood fibres as reinforcements in natural fibre composites: structure, properties, processing and applications. in *Natural Fibre Composites* 3–65 (Woodhead Publishing, 2014). doi:10.1533/9780857099228.1.3.
31. Chung, D. D. L. Electromagnetic interference shielding effectiveness of carbon materials. *Carbon* **39**, 279–285 (2001).
32. mahboubizadeh, S., Sadeq, A., Arzaqi, Z., Ashkani, O. & Samadoghli, M. Advancements in fiber-reinforced polymer (FRP) composites: an extensive review. *Discov. Mater.* **4**, 22 (2024).
33. Elena Bekyarova. Chemical Modification of Epitaxial Graphene: Spontaneous Grafting of Aryl Groups. *ACS Publ.* https://pubs.acs.org/doi/abs/10.1021/ja8057327 (2009).
34. Koronis, G., Silva, A. & Fontul, M. Green composites: A review of adequate materials for automotive applications. *Compos. Part B Eng.* **44**, 120–127 (2013).
35. Menard, K. P. *Dynamic Mechanical Analysis: A Practical Introduction, Second Edition*. (CRC Press, Boca Raton, 2008). doi:10.1201/9781420053135.
36. Kim, D. (Dae-W., Hennigan, D. J. & Beavers, K. D. Effect of fabrication processes on mechanical properties of glass fiber reinforced polymer composites for 49 meter (160 foot) recreational yachts. *Int. J. Nav. Archit. Ocean Eng.* **2**, 45–56 (2010).
37. Daniel, I. M., Ishai, O., Daniel, I. M. & Ishai, O. *Engineering Mechanics of Composite Materials*. (Oxford University Press, Oxford, New York, 2005).
38. *Engineering Mechanics of Composite Materials*. (Oxford University Press, New York, 2006).
39. Thiagarajan, S. & Munusamy, R. Experimental and numerical study of composite sandwich panels for lightweight structural design. *Int. J. Crashworthiness* https://www.tandfonline.com/doi/abs/10.1080/13588265.2020.1838178 (2022).
40. Affdl, J. C. H. & Kardos, J. L. The Halpin-Tsai equations: A review. https://doi.org/10.1002/pen.760160512 doi:10.1002/pen.760160512.
41. Hashin, Z. Failure Criteria for Unidirectional Fiber Composites. https://doi.org/10.1115/1.3153664 doi:10.1115/1.3153664.
42. Atif, R., Shyha, I. & Inam, F. Mechanical, Thermal, and Electrical Properties of Graphene-Epoxy Nanocomposites—A Review. *Polymers* **8**, (2016).
43. Silvestre, J., Silvestre, N. & de Brito, J. Polymer nanocomposites for structural applications: Recent trends and new perspectives. *Mech. Adv. Mater. Struct.* **23**, 1263–1277 (2016).
44. Akmal Zia, A. *et al.* Impact Resistance of 3D-Printed Continuous Hybrid Fiber-Reinforced Composites. *Polymers* **15**, 4209 (2023).
45. Khan, M. & Karthikeyan, R. Tensile and flexural behavior of synthetic and hybrid natural fiber composites for lightweight applications - Ramachandran - 2025 - Polymer Composites - Wiley Online Library. **46**, (2025).
46. Mirzapour, M., Cousin, P., Robert, M. & Benmokrane, B. Dispersion Characteristics, the Mechanical, Thermal Stability, and Durability Properties of Epoxy Nanocomposites Reinforced with Carbon Nanotubes, Graphene, or Graphene Oxide. *Polymers* **16**, (2024).
47. Hsissou, R. *et al.* Polymer composite materials: A comprehensive review. *Compos. Struct.* **262**, 113640 (2021).

